Channel Estimation Based on Deep Learning in Vehicle-to-Everything Environments

Jing Pan, Hangguan Shan, *Member, IEEE*, Rongpeng Li, *Member, IEEE*, Yingxiao Wu, Weihua Wu, and Tony Q. S. Quek, *Fellow, IEEE*

***Abstract*— Channel estimation in vehicle-to-everything (V2X) communications is a challenging issue due to the fast time-varying and non-stationary characteristics of wireless channel. To grasp the complicated variations of channel with limited number of pilots in the IEEE 802.11p systems, data pilot-aided (DPA) channel estimation has been widely studied. However, the error propagation in the DPA procedure, caused by the noise and the channel variation within adjacent symbols, limits the performance seriously. In this letter, we propose a deep learning based channel estimation scheme, which exploits a long short-term memory network followed by a multilayer perceptron network to solve the error propagation issue. Simulation results show that the proposed scheme outperforms currently widely-used DPA schemes for the IEEE 802.11p-based V2X communications.**

***Index Terms*— Channel estimation, data pilot-aided, IEEE 802.11p, deep learning.**

I. Introduction

In recent years, vehicle-to-everything (V2X) communication, as a core technology of intelligent transportation system, has attracted significant research attention for its potential of timely providing traffic information and supporting application services among vehicles [1], [2]. The IEEE 802.11p standard, also known as dedicated short range communication standard (DSRC) which is one of the competitive technologies for realizing V2X communication, has been widely studied. However, due to the highly mobile and relatively complex communication environments, channel estimation is a challenging issue with the pre-defined pilot pattern in the IEEE 802.11p standard. Conventional channel estimation schemes fail to yield satisfied results with such limited pilots in practical environments [3]. On the other hand, to guarantee spectral efficiency, it is unacceptable to insert more pilots in a packet.

To tackle the problem incurred by insufficient number of pilots, many researchers resort to the data pilot-aided (DPA) method of which the basic idea is utilizing the demapped data symbols as data pilots for channel estimation. However, applying such channel estimates to the equalization of a new symbol directly leads to the error propagation issue, which is mainly originated from the channel noise and channel variation within two adjacent symbols, thus influencing the transmission reliability significantly. The spectral temporal averaging (STA) scheme proposed in [4] improves the performance by averaging estimated channels in both time and frequency domains. The constructed data pilot (CDP) scheme [5] utilizes the correlation characteristics of channels within two adjacent symbols to judge the reliability of channel estimates and then decide whether or not to update the channels. By utilizing the demapped symbols to construct the data pilots, both the STA and CDP schemes have low computational complexity but are highly influenced by the reliability of data pilots. In contrast, DPA schemes based on decoded symbols as discussed in [6] relieve this issue but at the cost of the additional decoding delay and increased computational complexity.

Recently, deep learning techniques, which can extract the inherent characteristics from a large amount of data, have been applied to facilitate V2X communications. Utilizing a dense block pilot placement rather than DPA, the ChanEstNet network, consisting of a convolutional neural network and a bidirectional long short-term memory (LSTM) network, is designed to estimate channel in a high-speed environment [7]. The autoencoder (AE) based DPA scheme proposed in [8] uses an AE network to learn channel characteristics in the frequency domain for channel reconstruction and noise cancellation, and exhibits an obvious gain over the STA and CDP schemes. Gizzini *et al.* propose to combine STA and deep neural network (DNN) (named STA-DNN) to improve the channel estimates output by the STA scheme [9], which also reduces the computational complexity as compared with the AE scheme. Yet, the effect of channel variation is neglected by the AE scheme and can be impacted by the accuracy of the STA output for the STA-DNN scheme.

In this letter, we propose a deep learning based DPA channel estimation scheme for the IEEE 802.11p system. It combines the DPA procedure and neural network composed of two parts, namely an LSTM network and a multilayer perceptron (MLP) network, for learning the channel time and frequency correlation, respectively. By the DPA procedure, we update the channel estimates in each symbol, which solves the problem of insufficient number of pilots and provides more useful channel information for the neural network. On the other hand, by the neural network, which tracks channel variation and mitigates noise, we compensate the error of the DPA procedure efficiently. Simulation results show that the proposed scheme exhibits better performance than the previous DPA schemes especially for transmitting large-length packets with high-order modulation schemes and/or in fast time-varying channels.

II. System Model

In this section, we briefly introduce the physical layer of the IEEE 802.11p standard and analyze the DPA procedure.

Manuscript received December 9, 2020; revised January 21, 2021; accepted February 2, 2021. Date of publication February 16, 2021; date of current version June 10, 2021. This work was supported in part by the NSFC under Grants 61771427, U1709214, and 62027805, and in part by the SUTD-ZJU IDEA Grant for Visiting Professor ZJUVP1800104 and SUTD-ZJU Seed Grant SUTD-ZJU (SD) 201909. The associate editor coordinating the review of this letter and approving it for publication was M. Chafii. *(Corresponding author: Hangguan Shan.)*

Jing Pan, Hangguan Shan, and Rongpeng Li are with the College of Information Science and Electronic Engineering, Zhejiang University, Hangzhou 310027, China (e-mail: hshan@zju.edu.cn).

Yingxiao Wu is with the Zhejiang Laboratory, Hangzhou 310000, China.

Weihua Wu is with the School of Telecommunication Engineering, Xidian University, Xi'an 710126, China.

Tony Q. S. Quek is with the Pillar of Information Systems Technology and Design, Singapore University of Technology and Design, Singapore 487372.

Digital Object Identifier 10.1109/LCOMM.2021.3059922

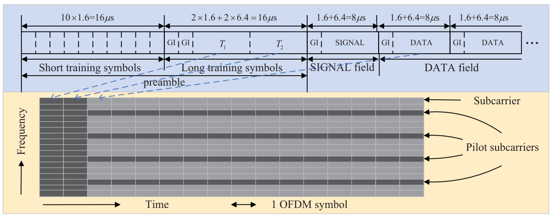

Fig. 1. IEEE 802.11p packet structure.

A. Pilot Pattern of IEEE 802.11p

The IEEE 802.11p physical layer is based on orthogonal frequency division multiplexing (OFDM) technology with 64-point fast fourier transformation in 5.9GHz carrier frequency with 8μs OFDM symbol duration. As shown in Fig. 1, each data packet consists of the preamble including short and long training symbols, SIGNAL field, and DATA field. The SIGNAL field conveys packet information (e.g., modulation scheme, coding rate, and data length) and the DATA field carries payload with data symbols. For each OFDM symbol, there are 64 subcarriers with an index set $\mathcal{S}_{\mathrm{N}} = \{-32, -31, \ldots, 31\}$, including 4 pilot subcarriers, 12 empty subcarriers, and 48 data subcarriers with index sets $\mathcal{S}_{\mathrm{P}} = \{-21, -7, 7, 21\}$, $\mathcal{S}_{\mathrm{E}} = \{-32,\ldots,-27, 0, 27,\ldots, 31\}$, and $\mathcal{S}_{\mathrm{D}} = \mathcal{S}_{\mathrm{N}} \cap (\mathcal{S}_{\mathrm{P}} \cup \mathcal{S}_{\mathrm{E}})^{\mathrm{C}}$, respectively, where $(\cdot)^{\mathrm{C}}$ means the complementary set.

For simplicity of representation, we ignore the SIGNAL field and let l represent the index of the OFDM symbols in the DATA field. The pilot pattern is shown in Fig. 1, including two parts, namely two long training symbols T_1 and T_2 in the preamble and pilots in the four pilot subcarriers. Assuming that channel is quasi-stationary, i.e., the channel does not change in one OFDM symbol duration but can vary from symbol to symbol, the received signal at the k-th subcarrier $Y_l(k)$ in the l-th OFDM symbol can be expressed as

$$Y_l(k) = H_l(k)X_l(k) + W_l(k) \tag{1}$$

where $H_l(k)$, $X_l(k)$, and $W_l(k)$ are the channel frequency response (CFR), transmitted signal, and complex Gaussian noise with zero mean and variance σ^2, respectively.

B. Analysis of the DPA Procedure

Without modification of the structure of IEEE 802.11p, the DPA channel estimation scheme tries to solve the problem of limited pilots, via amending the error of equalized data symbols from the demapping procedure to a certain extent and regarding the amended data symbols as pilots in each symbol for channel estimation. The DPA based scheme is flexible for the arbitrary packet length but its performance is impacted by the error propagation issue which is analyzed as follows.

Assuming that $\hat{X}_l(k)$ is the amended data symbol (i.e., data pilot) in the l-th OFDM symbol at the k-th subcarrier, the channel estimation calculated using the data pilot by the least square (LS) algorithm can be represented as

$$\hat{H}_l(k) = Y_l(k) \Big/ \hat{X}_l(k), \quad \forall k \in \mathcal{S}_{\mathrm{D}}. \tag{2}$$

If we apply the estimated CFR $\hat{H}_l(k)$ to obtain the transmitted data symbol in the next OFDM symbol directly by zero-forcing equalization as

$$\hat{X}_{l+1}(k) = Q\left(Y_{l+1}(k) \Big/ \hat{H}_l(k)\right), \quad \forall k \in \mathcal{S}_{\mathrm{D}} \tag{3}$$

where $Q(\cdot)$ denotes the operation mapping the equalized symbol to the closest constellation point, the error between the true CFR $H_{l+1}(k)$ and the estimated CFR $\hat{H}_l(k)$ will influence the reliability of data pilot $\hat{X}_{l+1}(k)$. The error consists of two parts, the channel estimation error between $\hat{H}_l(k)$ and $H_l(k)$ in the LS algorithm due to the additive noise in $Y_l(k)$, and the error by channel variation between $H_l(k)$ and $H_{l+1}(k)$ influenced by the Doppler shift. Therefore, it is imperative to find an error compensation method for the DPA procedure, so as to improve the accuracy of channel estimation and solve the channel variation problem.

III. Proposed Scheme

In this section, we introduce the proposed channel estimation scheme to compensate the error efficiently.

A. Neural Network Design

To address the error propagation issue, we design a novel neural network for tracking channel and mitigating noise. It is composed of an LSTM network and an MLP network, of which the structure and function are detailed as follows.

1) LSTM Network: Firstly, we employ the LSTM network, which is one of recurrent neural networks (RNNs) well known for time series prediction [10], to track channel. Assume each packet has L OFDM symbols indexed by $l \in \{1, 2, \ldots, L\}$. As shown in Fig. 2, one LSTM unit is in charge of dealing with channel estimation for demodulating one OFDM symbol. So, the number of LSTM units equals the number of the OFDM symbols in the packet. For the l-th OFDM symbol, we let the estimated CFRs in the last OFDM symbol and the current CFRs in the pilot subcarriers as the input of the corresponding LSTM unit. To facilitate channel estimation in the LSTM unit, we preprocess complex-valued CFRs by extracting their real part and imaginary part. So, the input vector $\mathbf{x}_l \in \mathbb{R}^{(2|\mathcal{S}_{\mathrm{D}}|+4|\mathcal{S}_{\mathrm{P}}|)\times 1}$ of the LSTM unit can be written as $\mathbf{x}_l = \left[\mathrm{Re}\left(\left[\hat{H}_{l-1}(k_1)\right]\right), \mathrm{Re}\left(\left[\hat{H}_l(k_2)\right]\right), \mathrm{Im}\left(\left[\hat{H}_{l-1}(k_1)\right]\right), \mathrm{Im}\left(\left[\hat{H}_l(k_2)\right]\right)\right]^{\mathrm{T}}$, where $k_1 \in \mathcal{S}_{\mathrm{D}} \cup \mathcal{S}_{\mathrm{P}}$ and $k_2 \in \mathcal{S}_{\mathrm{P}}$. Expect for $\mathbf{x}_l$, hidden state $\mathbf{h}_{l-1} \in \mathbb{R}^{p\times 1}$ and cell state $\mathbf{c}_{l-1} \in \mathbb{R}^{p\times 1}$ from the last LSTM unit are also the input of the current LSTM unit, with p being the hidden layer dimension of the LSTM unit.

The calculation of the cell state and the hidden state simply follows the normal process of LSTM network as follows

$$\mathbf{c}_l = \mathbf{f}_l \odot \mathbf{c}_{l-1} + \tilde{\mathbf{c}}_l \odot \mathbf{i}_l, \quad \mathbf{h}_l = \mathbf{o}_l \odot \tanh(\mathbf{c}_l) \tag{4}$$

where $\odot$ is the Hadamard product, and $\mathbf{f}_l, \tilde{\mathbf{c}}_l, \mathbf{i}_l$, and $\mathbf{o}_l \in \mathbb{R}^{p\times 1}$ are the forget gate, candidate cell, input gate, and output gate of the LSTM unit, respectively. They can be calculated with their own hidden weight matrix $\mathbf{W}_j \in \mathbb{R}^{p\times p}$, input weight matrix $\mathbf{V}_j \in \mathbb{R}^{p\times(2|\mathcal{S}_{\mathrm{D}}|+4|\mathcal{S}_{\mathrm{P}}|)}$, and bias vector $\mathbf{b}_j \in \mathbb{R}^{p\times 1}$, $j \in \{\mathrm{f}, \mathrm{c}, \mathrm{i}, \mathrm{o}\}$, as

$$\xi_l^j = \sigma_j\left(\mathbf{W}_j \mathbf{h}_{l-1} + \mathbf{V}_j \mathbf{x}_l + \mathbf{b}_j\right) \tag{5}$$

where $\xi_l^j = \mathbf{f}_l, \tilde{\mathbf{c}}_l, \mathbf{i}_l, \mathbf{o}_l$, if $j = \mathrm{f}, \mathrm{c}, \mathrm{i}, \mathrm{o}$, respectively, and σ_j is the sigmoid function if $j \neq \mathrm{c}$, otherwise it is the tangent function. It is noteworthy that, for tracking channel, $\mathbf{c}_l$ is a hidden structure saving long-term channel information, thus being the key of the output $\mathbf{h}_l$ of the current LSTM unit.

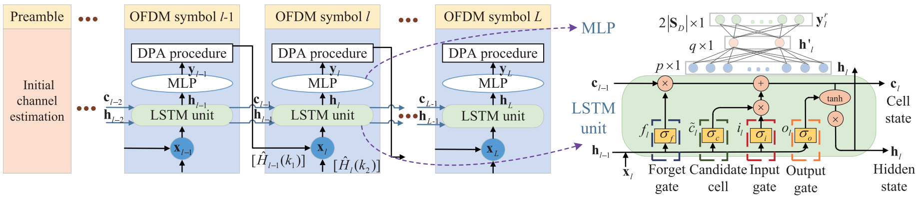

Fig. 2. Structure of the proposed network and channel estimation procedure.

2) MLP Network: Secondly, to increase the denoising ability of the neural network, we consider a two-layer MLP network following each LSTM unit. For the MLP network, the first layer processes the output of the LSTM unit by adopting the rectified linear unit (ReLU) function as the activation function and outputs vector $\mathbf{h}_l'$ with a reduced dimension $q(< \min\{p, 2|\mathcal{S}_{\mathrm{D}}|\})$ as channel frequency characteristics. Then, the second layer reconstructs the channel estimates and makes the final output $\mathbf{y}_l^{\mathrm{r}} = [\mathrm{Re}([\tilde{H}_l(k_3)]), \mathrm{Im}([\tilde{H}_l(k_3)])]^{\mathrm{T}}$ close to the real channel $\mathbf{y}_l = [\mathrm{Re}([H_l(k_3)]), \mathrm{Im}([H_l(k_3)])]^{\mathrm{T}}$, where $[\tilde{H}_l(k_3)]$ and $[H_l(k_3)]$, $k_3 \in \mathcal{S}_{\mathrm{D}}$, denote the compensated and real CFRs of data subcarriers, respectively. The MLP network can be described as

$$\mathbf{h}_l' = \max(\mathbf{W}'\mathbf{h}_l + \mathbf{b}_l', 0), \quad \mathbf{y}_l^{\mathrm{r}} = \mathbf{W}''\mathbf{h}_l' + \mathbf{b}_l'' \tag{6}$$

where $\mathbf{W}' \in \mathbb{R}^{q\times p}$, $\mathbf{W}'' \in \mathbb{R}^{2|\mathcal{S}_{\mathrm{D}}|\times q}$, $\mathbf{b}' \in \mathbb{R}^{q\times 1}$, $\mathbf{b}'' \in \mathbb{R}^{2|\mathcal{S}_{\mathrm{D}}|\times 1}$ are weight matrices and bias vectors, respectively, determined in the training process by minimizing the mean squared error (MSE) between the real CFRs $[H_l(k_3)]$ and compensated CFRs $[\tilde{H}_l(k_3)]$

$$\mathrm{MSE} = \frac{1}{N_{\mathrm{train}} L |\mathcal{S}_{\mathrm{D}}|} \sum_{N_{\mathrm{train}}} \sum_{l=1}^{L} \sum_{k_3\in\mathcal{S}_{\mathrm{D}}} \left\| H_l(k_3) - \tilde{H}_l(k_3) \right\|^2$$

with N_{train} denoting the number of the training packets.

Remark 1: The LSTM network utilizes the historical channel information to learn channel correlation in the time domain, while the MLP network extracts channel characteristics and reconstructs channel in the frequency domain. Benefitting from the proposed structure, both the time and frequency characteristics of the channel can be well learned for tracking channel variation as well as mitigating noise.

B. Deep Learning Based Channel Estimation

Then, we employ the proposed LSTM-MLP network in the DPA scheme which consists of three steps including initial channel estimation, error compensation, and DPA procedure. We introduce these steps in order as follows.

1) Initial Channel Estimation: In the first step, we utilize the two long training symbols in the preamble to obtain the initial channel estimation and the estimated CFR at the k-th carrier is calculated using the LS algorithm as

$$\hat{H}_0(k_1) = (Y_{T_1}(k_1) + Y_{T_2}(k_1))/2X(k_1) \tag{7}$$

where $X(k_1)$, $k_1 \in \mathcal{S}_{\mathrm{D}} \cup \mathcal{S}_{\mathrm{P}}$ is the predefined frequency domain long training symbol, and Y_{T_1} and Y_{T_2} represent the received signals.

2) Error Compensation: After obtaining the estimated CFRs in the last OFDM symbol, we use the LSTM-MLP network to compensate error as

$$\left[\tilde{H}_l(k_3)\right] = f_{\mathrm{LSTM-MLP}}(\theta; \mathbf{x}_l) \tag{8}$$

where θ denotes the parameters of the LSTM-MLP network, and $f_{\mathrm{LSTM-MLP}}(\theta; \mathbf{x}_l)$ represents of the process of the LSTM-MLP network given in (4)-(6).

3) DPA Procedure: Then $\tilde{H}_l(k_3)$ is utilized for equalization and the transmitted signal is determined as

$$\hat{X}_l(k_3) = Q(Y_l(k_3) \big/ \tilde{H}_l(k_3)), \quad \forall k_3 \in \mathcal{S}_{\mathrm{D}}. \tag{9}$$

Afterwards, we update the channel using the data pilots as

$$\hat{H}_l(k_3) = Y_l(k_3) \big/ \hat{X}_l(k_3), \quad \forall k_3 \in \mathcal{S}_{\mathrm{D}} \tag{10}$$

and deliver it to calculate the CFRs of the next OFDM symbol. Benefitting from the DPA procedure, the neural network obtains the reliable channel information as input.

Remark 2: Different from the conventional DPA schemes [4], [5], [8], [9], when demodulating each OFDM symbol, we employ error compensation before the DPA procedure and take the current channel estimates in the pilot subcarriers as part of the input, thus estimating the current channel as accurately as possible before use it for equalization.

C. Computational Complexity Analysis

For the complexity of the proposed scheme, similar to [9] we analyze the number of real-valued mathematical operations including multiplication/division and summation/subtraction needed to estimate the channel for one received OFDM symbol. First, for the initial channel estimation, according to (7) we need one complex-valued summation and one complex-real-valued division to estimate CFR for one subcarrier, because the long training symbols are binary phase shift keying (BPSK) modulated and the real-valued multiplication for $2X(k_1)$ in (7) can be calculated offline. So, the total number of real-valued multiplications/divisions and real-valued summations/subtractions for estimating all subcarriers in $\mathcal{S}_{\mathrm{D}} \cup \mathcal{S}_{\mathrm{P}}$ are $2(|\mathcal{S}_{\mathrm{D}}|+|\mathcal{S}_{\mathrm{P}}|)$ and $2(|\mathcal{S}_{\mathrm{D}}|+|\mathcal{S}_{\mathrm{P}}|)$, respectively. Second, for error compensation, we analyze the online computational complexity of the neural networks in terms of the required number of the real-valued multiplications and summations when computing the activation of all neurons in all layers. For the LSTM network, according to (5), to obtain $\mathbf{f}_l$, $\tilde{\mathbf{c}}_l$, $\mathbf{i}_l$, or $\mathbf{o}_l$, the required number of real-valued multiplications and summations are both $p^2 + p(2|\mathcal{S}_{\mathrm{D}}| + 4|\mathcal{S}_{\mathrm{P}}|)$, due to two matrix-vector multiplications and two vector summations. Besides, to derive the hidden state and cell state by (4), there are three Hadamard products and one vector summation, leading to $3p$ real-valued multiplications and p real-valued summations. For the MLP network, there are one matrix-vector multiplication and one vector summation for each layer according to (6), so the number of the real-valued multiplications and that of the real-valued summations for the two-layer MLP are both $pq + 2|\mathcal{S}_{\mathrm{D}}|q$. So, there are $4[p(2|\mathcal{S}_{\mathrm{D}}| + 4|\mathcal{S}_{\mathrm{P}}|) + p^2] + 3p + pq + 2|\mathcal{S}_{\mathrm{D}}|q$ real-valued multiplications and $4[p(2|\mathcal{S}_{\mathrm{D}}| + 4|\mathcal{S}_{\mathrm{P}}|) + p^2] + p + pq + 2|\mathcal{S}_{\mathrm{D}}|q$ real-valued summations for error compensation in the proposed scheme. Finally, according

TABLE I

V2V CHANNEL GENERATION PARAMETERS IN SUBURBAN ENVIRONMENT

Parameter	Physical meaning	Mean	Standard deviation
D	Initial distance between receiver and transmitter	400 m	0 m
$(\psi_{\mathrm{A}}^{\mathrm{T}}, \psi_{\mathrm{E}}^{\mathrm{T}})$	Azimuth and elevation angles of transmitter array broadside	$(\frac{\pi}{3}, \frac{\pi}{4})$ rad	$(0, 0)$ rad
$(\psi_{\mathrm{A}}^{\mathrm{R}}, \psi_{\mathrm{E}}^{\mathrm{R}})$	Azimuth and elevation angles of receiver array broadside	$(\frac{\pi}{4}, \frac{\pi}{4})$ rad	$(0, 0)$ rad
$\sigma_{\mathcal{T}}$	Delay spread of cluster virtual delays	-6.39 dB	0.63 dB
$r_{\mathcal{T}}$	Delay scalar of cluster virtual delays	2.5	0
$std[\phi_n^{\mathrm{A}}]$, $std[\phi_n^{\mathrm{E}}]$, $std[\varphi_n^{\mathrm{A}}]$, $std[\varphi_n^{\mathrm{E}}]$	Angular parameters of cluster n	$38.8, 47,$ $38.2, 23.6$	$0, 0,$ $0, 0$
D_n^{R}	Initial distance between cluster n and receiver array center	10 m	15 m
D_n^{T}	Initial distance between cluster n and transmitter array center	10 m	20 m
M_n	Number of rays within cluster n	15	15
λ_{G}	Generation rate of cluster	32	0
λ_{R}	Recombination rate of cluster	4	0
$D_{\mathrm{c}}^{\mathrm{s}}$	Scenario-dependent coefficient describing space correlation	30 m	0 m
P_{F}	Percentage of moving clusters	0.3	0
v_{c}	Mean cluster velocity	0.5 m/s	0 m/s

to (9) and (10), for each data subcarrier we need one complex-valued division for both data pilot acquisition and data pilot based channel estimation. So, there are $16|\mathcal{S}_{\mathrm{D}}|$ real-valued multiplications/divisions and $6|\mathcal{S}_{\mathrm{D}}|$ real-valued summations/subtractions in the DPA procedure.

IV. SIMULATION RESULTS

In this section, we present simulation results to verify the performance of the proposed channel estimation scheme.

A. Simulation Setting

To train the parameters of the LSTM-MLP network, we obtain the training dataset by using the 3-D non-stationary 5G wireless channel model proposed in [11]. It is a geometry-based stochastic model built on the WINNER II channel model, which can simulate small-scale fading for many scenarios, e.g., massive MIMO, V2X, high-speed train, and mmWave, by setting proper channel parameters. Table I lists the main channel parameters that we use to simulate for a non-line-of-sight (NLOS) vehicle-to-vehicle (V2V) environment and the meaning of the parameters are the same in [11]. To improve generalization capability, we generate the channel of the training dataset under different transmitter velocities v_{T}'s and receiver velocities v_{R}'s, varying from 10 m/s (i.e., 36 km/h) to 40 m/s (i.e., 144 km/h) with a granularity of 10 m/s. It is noteworthy that for the training process we do not consider the impact of noise. Further, in the simulation we set the transmitter and receiver antenna number to 1 and adopt the omnidirectional antenna pattern. Besides, Table II shows the detailed parameters of the proposed LSTM-MLP architecture and those used in the training phase.

B. BER Performance

To analyze the effect of each cornerstone of the proposed scheme, we firstly compare the bit error rate (BER) performance of the proposed scheme with two baseline schemes: the first one adopts LSTM-MLP for channel estimation but without using the DPA procedure; the second one adopts LSTM and DPA for channel estimation but without using MLP. Fig. 3 shows the BER results for 16QAM with the testing channel generated also by the channel model in [11], for two vehicles moving with the same direction at transmitter velocity $v_{\mathrm{T}} = 108\,\mathrm{km/h}$ and receiver velocity $v_{\mathrm{R}} = 72\,\mathrm{km/h}$. As compared with the first baseline, the proposed scheme has superior performance in a medium or high signal-to-noise

TABLE II

PARAMETERS USED IN THE TRAINING PHASE

Parameter	Value
LSTM-MLP (hidden layers, neurons per layer)	(2, 128-40)
Number of epochs	200
Number of training samples, validating samples	12000, 4000
Number of testing samples	2000
Batch size	128
Optimizer	Adam
Learning rate, drop period, factor	0.01, 20, 0.8
Number OFDM symbols per packet	50

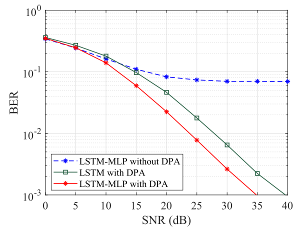

Fig. 3. Cornerstone analysis of the proposed scheme.

ratio (SNR) region (e.g., ≥ 15 dB), and the performance gap increases with the SNR value, because DPA provides more and more reliable channel estimates when the channel condition improves. Besides, as compared with the second baseline, though adding MLP following the LSTM unit, the LSTM-MLP network learns the channel characteristics better and achieves, for example, 5 dB gain for BER at 10^{-3}.

To further verify the performance of the proposed scheme, we also compare its BER performance with other DPA schemes including STA [4], CDP [5], AE [8], and STA-DNN [9]. Fig. 4(a) shows the BER results for 16QAM and 64QAM when vehicles move with the opposite directions but at untrained velocities $v_{\mathrm{T}} = 150$ km/h and $v_{\mathrm{R}} = 150$ km/h. In the simulation, for the AE and STA-DNN schemes, we adopt the 40-20-40 and 15-10-15 hidden layer dimensions for the AE and DNN networks, respectively. Besides, the STA-DNN scheme is trained at SNR equal to 30 dB [9]. It can be seen that the deep learning based schemes, including AE, STA-DNN, and the proposed one, outperform the conventional DPA schemes such as CDP and STA. Because the amending capability for equalized data symbols depends on the modulation scheme the error propagation issue is severer in the 64QAM case. But, it is observed from Fig. 4(a) that, the gap between the proposed scheme and the AE or STA-DNN scheme at any BER performance for 64QAM

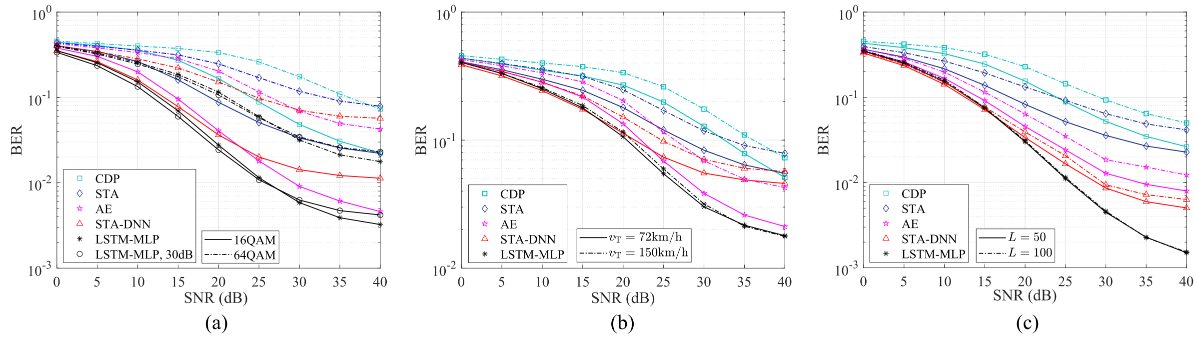

Fig. 4. BER comparison: (a) under different modulation schemes when vehicles move with the opposite directions and untrained velocities $v_{\mathrm{T}} = 150$ km/h and $v_{\mathrm{R}} = 150$ km/h; (b) for 64QAM when vehicles move with the opposite directions and untrained different transmitter velocities given receiver velocity $v_{\mathrm{R}} = 150$ km/h; (c) for 16QAM under different packet lengths in the V2VEO scenario generated by channel model [12] under maximum Doppler shift 1200 Hz.

is larger than 16QAM, implying that the proposed scheme has superior error compensation effect due to the channel tracking function of the proposed LSTM-MLP network. It is noteworthy that the performance gain of the proposed scheme over the AE or STA-DNN scheme is also at the cost of computational complexity. For example, with the test network setting it achieves about 3.3 (15) dB gain over the AE (STA-DNN) scheme for 16QAM at BER equal to 10^{-2}, but needs about 13 (30) times of real-valued multiplication/division or summation/subtraction operations than the AE (STA-DNN) scheme. As unearthed in [13] that the performance of neural networks highly depends on the SNR setting in the training phase, we also study the LSTM-MLP network by retraining it at SNR equal to 30 dB. One can notice that the proposed scheme performs relatively better in a low SNR region but worse in a high SNR region if training in a noisy condition.

To study the impact of Doppler shift, Fig. 4(b) compares different DPA schemes for 64QAM when vehicles move with the opposite directions but untrained velocity setting, where receiver velocity $v_{\mathrm{R}} = 150$ km/h and transmitter velocity v_{T} is 72 km/h and 150 km/h, respectively. One can notice that, as the transmitter velocity increases, the proposed scheme has least performance loss among all compared schemes. This is because, the LSTM network learns the channel time correlation efficiently, although it cannot completely eliminate the estimation error due to channel variation. On the contrary, when the transmitter velocity is larger, the AE scheme has an obvious performance loss, as it ignores the impact of channel variation. For the STA-DNN scheme, though its performance loss reduces, it still exists, because the scheme takes channel variation into account but its performance can be constrained by the accuracy of the STA output.

To study the impact of packet length on the proposed scheme, Fig. 4(c) shows the BER performance of diverse DPA schemes, tested with the channel in [12] for simulating the V2V expressway coming (V2VEO) scenario under maximum Doppler shift 1200 Hz. It is noteworthy that the LSTM-MLP network tested here is still the one trained with the channel generated according to [11]. It is verified from Fig. 4(c) that, the performance of each scheme becomes worse as the packet length increases. But, the proposed scheme has a less performance loss because it has better error compensation effect in each symbol, even the training dataset and test dataset are generated completely from two different models.

V. Conclusion

In this letter, we proposed a novel LSTM-MLP based channel estimation scheme with DPA method for the IEEE 802.11p standard in the fast time-varying vehicle channel environments. To solve the error propagation issue caused by noise and channel variation in the DPA procedure, we use the LSTM-MLP network to mitigate noise and track channel. Simulation results show the effectiveness of the proposed scheme in fast time-varying channels, especially for high-order modulation schemes or large-length packets. For the future work, we will study how to reduce the computational complexity of the proposed scheme while achieving a good performance via exploiting attention mechanisms to learn inherent channel characteristics over a tunable number of coherence intervals [14].

References

[1] L. Liang *et al.*, "Vehicular communications: A physical layer perspective," *IEEE Trans. Veh. Technol.*, vol. 66, no. 12, pp. 10647–10659, Dec. 2017.

[2] Y. Bi *et al.*, "A multi-hop broadcast protocol for emergency message dissemination in urban vehicular ad hoc networks," *IEEE Trans. Intell. Transp. Syst.*, vol. 17, no. 3, pp. 736–750, Mar. 2016.

[3] L. Bernado *et al.*, "Physical layer simulation results for IEEE 802.11p using vehicular non-stationary channel model," in *Proc. IEEE Int. Conf. Commun. Workshops*, May 2010, pp. 1–5.

[4] J. A. Fernandez *et al.*, "Performance of the 802.11p physical layer in vehicle-to-vehicle environments," *IEEE Trans. Veh. Technol.*, vol. 61, no. 1, pp. 3–14, Jan. 2012.

[5] Z. Zhao *et al.*, "Channel estimation schemes for IEEE 802.11p standard," *IEEE Intell. Transp. Syst. Mag.*, vol. 5, no. 4, pp. 38–49, Oct. 2013.

[6] P. Alexander *et al.*, "Cooperative intelligent transport systems: 5.9-GHz field trials," *Proc. IEEE*, vol. 99, no. 7, pp. 1213–1235, Jul. 2011.

[7] Y. Liao *et al.*, "ChanEstNet: A deep learning based channel estimation for high-speed scenarios," in *Proc. ICC-IEEE Int. Conf. Commun. (ICC)*, May 2019, pp. 1–6.

[8] S. Han *et al.*, "A deep learning based channel estimation scheme for IEEE 802.11p systems," in *Proc. ICC-IEEE Int. Conf. Commun. (ICC)*, May 2019, pp. 1–6.

[9] A. K. Gizzini *et al.*, "Deep learning based channel estimation schemes for IEEE 802.11p standard," *IEEE Access*, vol. 8, pp. 113751–113765, Jun. 2020.

[10] Y. Hua *et al.*, "Deep learning with long short-term memory for time series prediction," *IEEE Commun. Mag.*, vol. 57, no. 6, pp. 114–119, Jun. 2019.

[11] S. Wu *et al.*, "A general 3-D non-stationary 5G wireless channel model," *IEEE Trans. Commun.*, vol. 66, no. 7, pp. 3065–3078, Jul. 2018.

[12] G. Acosta-Marum and M. A. Ingram, "Six time- and frequency-selective empirical channel models for vehicular wireless LANs," *IEEE Veh. Technol. Mag.*, vol. 2, no. 4, pp. 4–11, Dec. 2007.

[13] A. K. Gizzini *et al.*, "Enhancing least square channel estimation using deep learning," in *Proc. IEEE 91st Veh. Technol. Conf. (VTC-Spring)*, May 2020, pp. 1–5.

[14] P. Dong *et al.*, "Deep CNN-based channel estimation for mmWave massive MIMO systems," *IEEE J. Sel. Topics Signal Process.*, vol. 13, no. 5, pp. 989–1000, Sep. 2019.